Proc. Natl. Acad. Sci. USA
Vol. 93, pp. 6421–6424, June 1996
Developmental Biology

Targeted mutation of *Ncam* to produce a secreted molecule results in a dominant embryonic lethality

(neural cell adhesion molecule/homologous recombination/mouse/dominant lethal)

JOSEPH E. RABINOWITZ, URS RUTISHAUSER, AND TERRY MAGNUSON*

Department of Genetics, Case Western Reserve University, 10900 Euclid Avenue, Cleveland, OH 44106-4955

Communicated by Anthony P. Mahowald, University of Chicago, Chicago, IL, March 8, 1996 (received for review December 8, 1995)

ABSTRACT **The neural cell adhesion molecule (NCAM) is a membrane-associated member of the immunoglobulin superfamily capable of both homophilic and heterophilic binding. To investigate the significance of this binding, a gene targeting strategy in embryonic stem (ES) cells was used to replace the membrane-associated forms of NCAM with a soluble, secreted form of its extracellular domain. Although the heterozygous mutant ES cells were able to generate low coat color chimeric mice, only the wild-type allele was transmitted, suggesting the possibility of dominant lethality. Analysis of chimeric embryos with high level of ES cell contribution revealed severe growth retardation and morphological defects by E8.5–E9.5. The second allele was also targeted, and embryos derived almost entirely from the homozygous mutant ES cells exhibited the same lethal phenotype as observed with heterozygous chimeras. Together, these results indicate that dominant lethality associated with the secreted NCAM does not require the presence of membrane-associated NCAM. Furthermore, the data indicate that potent bioactive cues or signals can be generated by NCAM.**

The neural cell adhesion molecule (NCAM) is a membrane-bound immunoglobulin superfamily glycoprotein that plays a role in cell–cell and cell–matrix adhesion through both its homophilic and heterophilic binding activity (1). Targeted mutations in the *Ncam* gene have been produced in embryonic stem (ES) cells to generate mutant mice in which the *in vivo* function of NCAM can be evaluated. The first two animals generated, a null mutation and a deletion of one of the major NCAM isoforms, were both viable and fertile, with no phenotype evident by casual observation (2, 3). However, more intensive analysis revealed localized and distinct defects in the central nervous system including the morphology of the subventricular zone, olfactory bulb, cerebellum, retina, and hippocampus (3). Other aspects of the phenotype remain to be discovered and studied, but also are likely to represent localized alterations in tissue structure.

In this study we employed the same genetic approach to a different purpose, namely to examine the effects of NCAM-binding events through the generation of a soluble and secreted form of the extracellular domain of the molecule. Furthermore, the use of homologous recombination to generate the secreted form has provided the opportunity to examine these effects in the absence of the membrane-associated forms. The findings indicate that abnormal NCAM expression is capable of generating drastic malformations that were not apparent from either the null or the NCAM180 isoform mutations (2, 3).

MATERIALS AND METHODS

Construction of Targeting Vectors and Generation of Chimeric Embryos. A 5.7-kb *Bam*HI *Ncam* genomic clone was isolated by standard methods from a 129/Sv λfixII mouse library (Stratagene) and cloned into a *Bgl*II site in the β-actin DT-A vector. This vector was digested with *Bcl*I, which removed a 500-bp fragment whose 5′ end was within exon 13 and the 3′ end downstream in the intron. A 2.0-kb *Bam*HI/*Bgl*II fragment containing the neomycin (Neo) cassette replaced the 500-bp *Bcl*I fragment. ES cells were electroporated with the Neo vector linearized with *Eco*RI and selected in Geneticin (GIBCO/BRL) (200 $\mu g/ml^{-1}$). The puromycin (Puro) vector was generated by digesting the Neo vector and the pgkpuropA vector with *Sph*I and isolating the 9.2-kb fragment from the Neo vector and a 1.6-kb fragment from the pgkpuropA vector. These fragments were ligated and orientation determined. ES cells previously targeted with the Neo vector were electroporated with the Puro vector linearized with *Eco*RI, and selected in Geneticin (200 $\mu g/ml^{-1}$) and puromycin (Sigma) (1 $\mu g/ml^{-1}$). Targeted clonal lines were injected either into blastocysts of the CF-1 or CD-1 strain, or into CD-1 precompacted eight-cell embryos. In some cases, chimeras were produced by aggregating CD-1 eight-cell embryos with targeted ES cells.

Table 1. Analysis of embryos injected with targeted ES cells

Gestational (cell line)	No. of embryos	Chimeric* embryos	Mutant phenotype/ high ES cell chimeras§
Heterozygous ES cells injected			
E10.5 (R1)†	61	13	4/4
E9.5 (R1)‡	54	13	2/2
E9.5 (CT1)‡	63	8	2/2
E8.5 (R1)	43	4	1/1
Homozygous ES cell injected			
E10.5 (R1)	12	ND	ND/2
E9.5 (R1)	35	11	5/5

ND, not determined.
*Chimerism was determined by Southern blot analysis.
†Multiple-targeted R1 lines demonstrated the mutant phenotype.
‡Tetraploid aggregations are included.
§Contribution over 90% as determined by scanning densitometry on a phosphoimager.

Differentiation and Analysis of ES Cells. Parental and homozygous targeted ES cells were grown as embryoid bodies (4) except that cells were plated on tissue culture plates coated with gelatin (0.1%) for protein isolation or on slides (Lab-Tek) coated with polyornithine and laminin for immunofluorescence. Cells were grown in F12 medium +N2 supplement (GIBCO/BRL). Soluble NCAM was isolated from cultures of differentiated ES cells (5). For immunofluorescence, cells were fixed in 4% paraformaldehyde (Fisher), incubated in polyclonal anti-NCAM antibody for 1 hr and in 2° antibody fluorescein isothiocyanate-conjugated goat anti-rabbit IgG

The publication costs of this article were defrayed in part by page charge payment. This article must therefore be hereby marked "*advertisement*" in accordance with 18 U.S.C. §1734 solely to indicate this fact.

Abbreviations: NCAM, neural cell adhesion molecule; ES, embryonic stem; E, embryonic day.

*To whom reprint requests should be addressed.

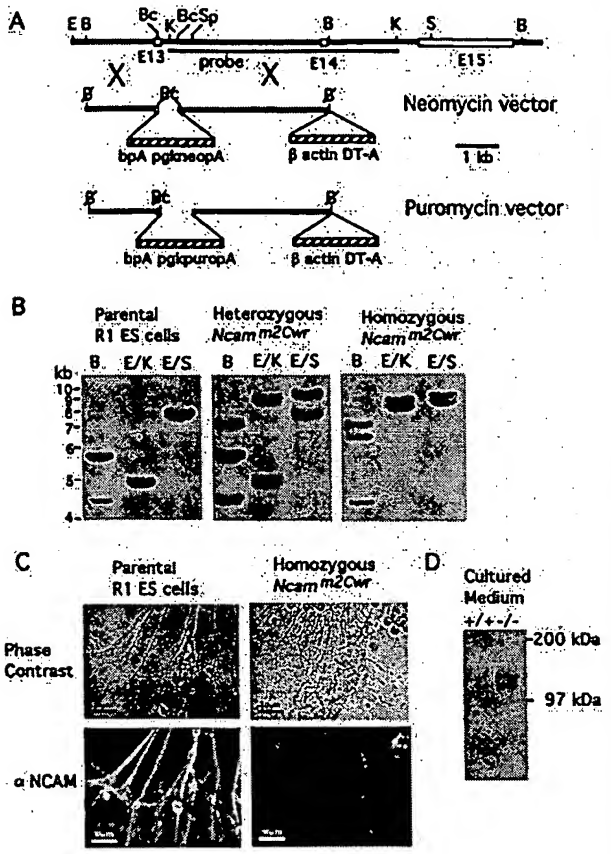

FIG. 1. Targeted disruption of the *Ncam* gene in D3 (7), R1 (8), and CT1 (C. LaMantia, and T.M., unpublished results) ES cells at exon 13 by homologous recombination. (*A*) Schematic restriction map of the endogenous *Ncam* locus around exon 13, the Neo targeting vector, and the Puro targeting vector. Thick black lines represent introns, open boxes represent exons, striped boxes represent the bovine growth hormone polyadenylation addition (bpA) site linked to the phosphoglycerate kinase neomycin polyadenylylation (pgkneopA) (9) or puromycin polyadenylylation (pgkpuropA) cassettes, and the β-actin diphtheria toxin A fragment (DT-A) (10) cassette. The Neo cassette replaces a 500-bp genomic fragment between two *Bcl*I sites, removing a *Kpn*I site, and the Puro cassette deletes 1 kb of genomic DNA extending from exon 13 *Bcl*I 5′ to the 3′ *Sph*I site. The targeting vectors were linearized with *Eco*RI. An internal probe, used to screen for homologous recombination events, is represented by a thin black line under the endogenous genomic map. Crossed letters are restriction sites destroyed during cloning. (*B*) Southern blot analysis of genomic DNA isolated from parental ES cells, heterozygous Neo vector targeted ES cells, and Neo/Puro vector targeted ES cells. The *Bam*HI digest resulted in two endogenous fragments (5.7 and 4.5 kb) due to the probe overlap of a *Bam*HI site. The *Eco*RI/*Kpn*I and *Eco*RI/*Sac*I digests showed endogenous band sizes of 4.8 kb and 8.2 kb, respectively. The *Bam*HI digest of the Neo vector targeted allele shows a size of 7.2 kb and a Puro vector targeted allele band size of 6.7 kb. The *Eco*RI/*Kpn*I digest of the Neo vector targeted allele shows a size of 8.7 kb, and a Puro vector targeted allele size of 8.2 kb. The *Eco*RI/*Sac*I digest of the Neo vector targeted allele shows a size of 9.7 kb and a Puro vector targeted allele shows a size of 9.2 kb. (*C*) Expression of cell surface NCAM by ES-derived neuronal cells as assessed by immunofluorescence microscopy with anti-NCAM antibody. Parental and homozygous targeted ES cells were induced to differentiate along a neuronal pathway by retinoic acid (4). Corresponding phase contrast images are shown above the fluorescence images. Note that the strong staining of cell bodies and neurites observed with cells derived from parental ES cells was completely absent with cells derived from homozygous mutant ES cells. (Bar = 30 μm.) (*D*) Soluble, secreted NCAM immunoprecipitated from medium of cultures of parental (+/+) and homozygous mutant (−/−) ES cells induced to differentiate with retinoic acid and then metabolically labeled with [^{35}S]methionine (Amersham). E, *Eco*RI; B, *Bam*HI; Bc, *Bcl*I; K, *Kpn*I; Sp, *Sph*I; S, *Sac*I; E13, exon 13; E14, exon 14; E15, exon 15.

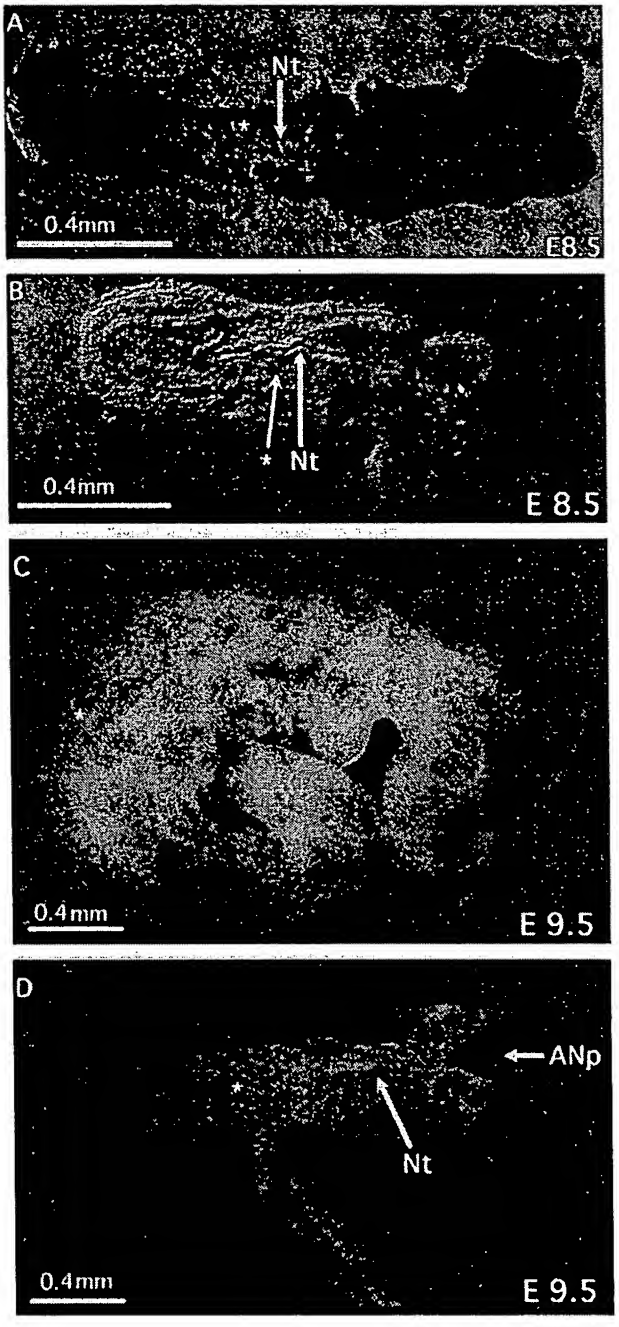

FIG. 2. Morphology of wild-type and chimeric mutant embryos with high ES cell contribution at E8.5 and E9.5. All embryos are shown with anterior to the left and posterior to the right. (*A*) Wild-type E8.5 embryo. Note that the straight neural tube and bilaterally symmetrical somites on either side of the neural tube. (*B*) Chimeric heterozygous embryo. Note that the neural tube is kinked and the somites are few in number and disorganized. (*C*) Wild-type E9.5 CD-1 embryo. Note that this embryo has completed turning, the cephalic neuropore has closed, and the branchial arches and limb development are normal. (*D*) Dorsal view of a chimeric homozygous embryo. Note that the cephalic neural folds have not closed, limb buds have not formed, and the neural tube is severely kinked. (Bar = 0.4 mm). Nt, neural tube; ANp, anterior neuropore; •, somite.

(Cappel) for 1 hr, and photographed using a Zeiss Axiophot with a 40× objective.

Preparation and Imaging of Embryos. Dissected embryos were fixed in 4% paraformaldehyde overnight at 4°C. The

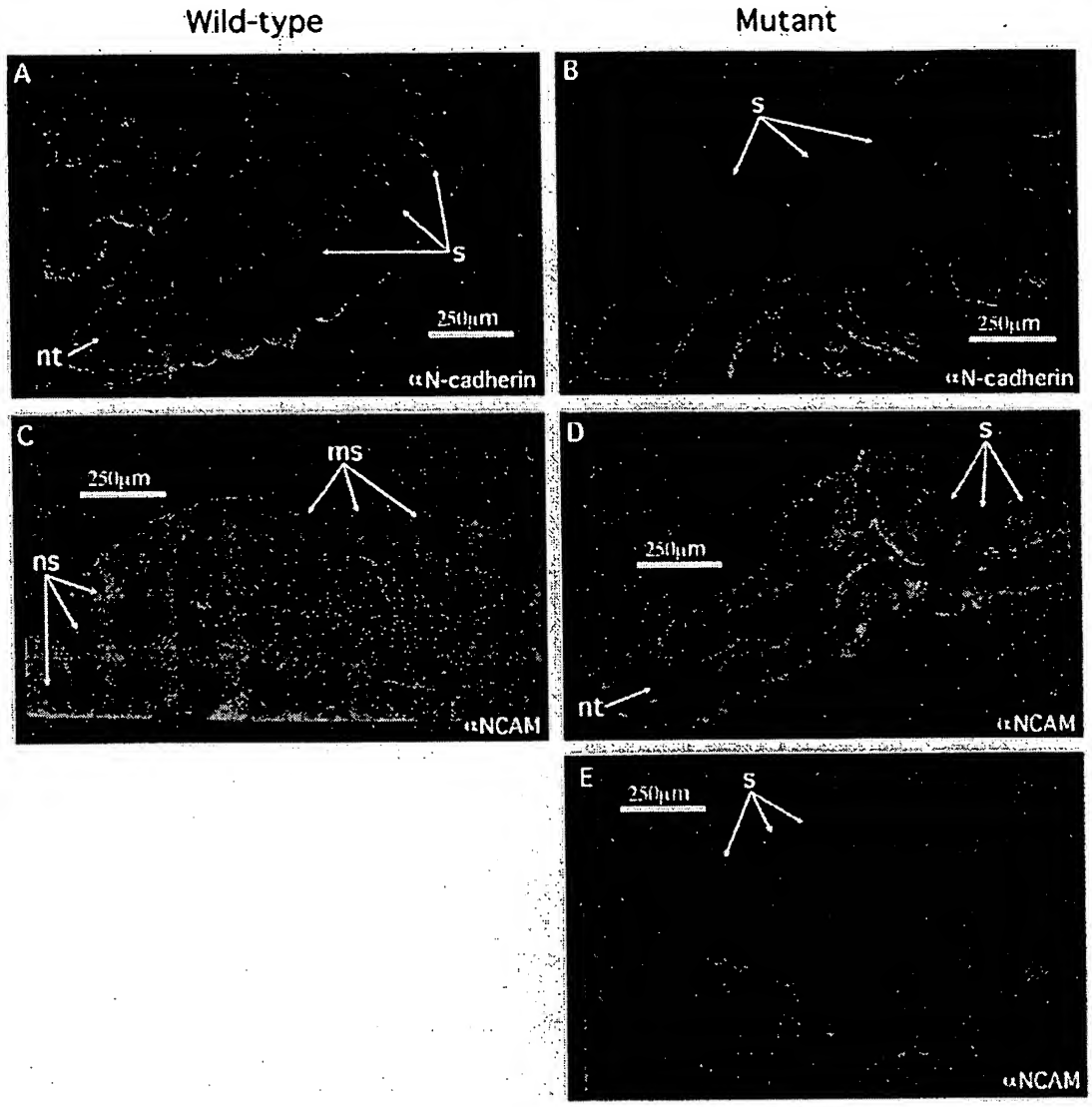

FIG. 3. Expression of N-cadherin and NCAM in wild-type and mutant chimeric embryos at E9.5. (*A* and *C*) Wild-type. (*B* and *E*) Homozygous mutant. (*D*) Heterozygous mutant. (*A* and *B*) N-cadherin expression. (*C–E*) NCAM expression. (Bar = 250 μm.) ns, nascent formed somite; ms, mature somite; nt, neural tube.

embryos were then washed in PBS and stored in methanol for from 24 hr to 2 weeks at 4°C. The embryos were rehydrated through an ethanol series into PBS and then washed twice for 30 min each. The embryos were incubated for 30 min in 1 M glycine (pH 7–8) and washed in PBS, then incubated in PBS plus 3% H_2O_2 for 10 min, followed by four washes (1 × PBS/0.2% BSA/0.1% Tween 20) 30 min each, and then placed in dilution buffer (1 × PBS/0.2% BSA/0.1% Tween 20/1% fetal calf serum) for 30 min, followed by antibody in dilution buffer overnight at 4°C. The embryos were washed in buffer 7 times for 30 min each, then in dilution buffer for 30 min. Next, they were incubated overnight with a fluorescein isothiocyanate-conjugated secondary antibody. The embryos were washed 7 times in antibody wash buffer and placed in glycerol on a depression well slide and stored at 4°C. Images were acquired using a Zeiss Axioplan microscope equipped with a Bio-Rad MRC-600 series laser scanning confocal imaging system. For each image up to 32 optical sections were superimposed. Red and blue colors were removed to generate the fluorescein isothiocyanate image. Confocal images were transferred to Adobe Photoshop (Adobe Systems, Mountain View, CA) and printed on a Kodak electric printer.

RESULTS AND DISCUSSION

Multiple independent-targeted clonal ES cell lines (6) carrying a Neo replacement in exon 13 (Fig. 1*A*) were isolated in three parental ES lines at an overall frequency of 1/35. These lines were confirmed to be heterozygous for the mutation by diagnostic Southern blot analysis (Fig. 1*B*). Exon 13 is a nonalternatively spliced exon coding for part of the second fibronectin type III repeat in the extracellular domain (11). This mutation results in a premature stop codon followed by a bovine growth hormone polyadenylylation signal. One of the mutant heterozygous lines was subjected to a second round of targeting using a puromycin replacement vector (Fig. 1*A*) to obtain a homozygous line. This was achieved at a frequency of 1/184 and was confirmed by diagnostic Southern blot analysis (Fig. 1*B*). NCAM was not present on the surface of homozygous mutant ES cells induced to differentiate along a neuronal lineage (Fig. 1*C*). By contrast, the culture medium from these neural cultures contained a secreted form of NCAM of the expected size (Fig. 1*D*).

Heterozygous ES cells were used to generate 13 live-born founder chimeras (11 male and 2 female). Each animal con-

tained a low contribution of ES cells as judged by coat color and Southern blot analysis (data not shown). Males were bred to C57BL/6 females, and 33 of 605 progeny were agouti. However, all of the progeny contained the wild-type *Ncam* allele. Although the mutant allele was determined to be present in testes by Southern blot analysis and in sperm by nested PCR (data not shown), this allele was not transmitted to viable offspring. These results suggested that fetuses carrying the mutation in the heterozygous state had died *in utero*.

To facilitate the investigation of this apparent dominant lethality, we created chimeric embryos with different levels of mutant ES contribution. Fetuses were dissected and analyzed between embryonic day (E) 8.5 and E10.5, the time at which NCAM begins to be expressed (12). Approximately 6% of the embryos were found to be growth delayed or undergoing resorption (Table 1), and this class of embryos contained greater than 90% ES cell contribution as shown by Southern blot analysis and scanning densitometry (data not shown). Moreover, the same degree of lethality was obtained with either heterozygous or homozygous ES cells and was observed with targeted clonal lines isolated from all three parental lines.

Abnormalities were first detected in chimeras with high ES cell contribution at E8.5. These embryos were truncated, and histologically the major initial defects were a reduced number of poorly formed somites and a kinking of the neural tube (Fig. 2 *A* and *B*). By E9.5, the mutant embryos exhibited an open anterior neuropore, small and irregular somites, and an absence of limb buds (Fig. 2 *C* and *D*). The abnormal differentiation of the mutant somites was also examined in terms of the expression patterns of N-cadherin and NCAM. In wild-type somites, N-cadherin expression was confined to the apical epithelial layer (Fig. 3*A*) (13), whereas in mutant somites a broad diffuse pattern was observed (Fig. 3*B*). With respect to NCAM in the heterozygote, which expresses both the membrane bound and secreted forms (Fig. 3*D*), the pattern in all mutant somites resembled the distribution seen in nascent somites of wild-type embryos (Fig. 3*C*, *left*). As expected for a soluble, secreted protein, the truncated NCAM in homozygous embryos resulted in a completely diffuse staining pattern throughout all tissues (Fig. 3*E*).

The null (2) and 180 isoform (3) mutations of NCAM both resulted in fertile, viable progeny with distinct, localized defects in several differentiated tissues. In contrast, the present study shows that secretion of the extracellular domain of NCAM results in a dominant embryonic lethality with gross abnormalities in somitogenesis already evident by the end of gastrulation. Thus, it would appear that potent signals leading to abnormal somitogenesis can be generated by the presence of NCAM in the extracellular environment. A similar phenotype was reported in *Xenopus* embryos injected with RNA encoding the NCAM180 isoform (14). Whereas the differences in the forms of the molecule and the method of experimental delivery make it difficult to compare these two studies directly, it would appear that similar signals can be produced by excessive expression of the extracellular domain in either a soluble or membrane-bound form. It may be noted that injection of RNA encoding only the extracellular domain of NCAM did not ellicit abnormal somitogenesis in the *Xenopus* embryo. However, this latter result may not be relevant because it appeared the truncated molecule was retained within the cytoplasm.

The fact that lethality was observed in the founder chimeras containing homozygous mutant ES cells, thus in the absence of membrane-bound NCAM, suggests that the secreted NCAM is producing this phenotype through a heterophilic- rather than a homophilic-binding mechanism. While we cannot rule out the possibility of a nonspecific toxicity of the soluble NCAM itself, NCAM has been reported to participate in specific heterophilic interactions with extracellular matrix components such as collagens (15), heparan sulfate (16, 17), and chondroitin sulfate (18) proteoglycans, and with membrane-associated signaling molecules such as the L1 adhesion molecule (19) and the fibroblast growth factor receptor (20). It is therefore tempting to speculate that the formation of somites from paraxial mesoderm in the mutant is compromised by abnormal heterophilic interactions of NCAM that either affect migration of mesenchymal cells through the extracellular matrix or perturb signals linked to somite differentiation.

We thank Lilly Yuzon for blastocyst injections. This work was supported in part by National Institutes of Health Grants to T.M. (HD26722), U.R. (HD18369 and EY06107), and J.E.R. (National Institutes of Health Training Grant HD07104-16).

1. Rutishauser, U. (1991) in *Receptors for Extracellular Matrix*, eds. McDonald, J. & Mecham, P. (Academic, San Diego), pp. 131–156.
2. Cremer, H., Lange, R., Christoph, A., Plomann, M., Vopper, G., Roes, J., Brown, R., Baldwin, S., Kraemer, P., Scheff, S., Barthels, D., Rajewsky, K. & Wille, W. (1994) *Nature (London)* **367**, 455–459.
3. Tomasiewicz, H., Ono, K., Yee, D., Thompson, C., Rutishauser, U. & Magnuson, T. (1993) *Neuron* **11**, 1163–1174.
4. Bain, G., Kitchens, D., Yao, M., Huettner, J. & Gottlieb, D. I. (1995) *Dev. Biol.* **168**, 342–357.
5. Bruses, J. L., Oka, S. & Rutishauser, U. (1996) *J. Neurosci.* **15**, 8310–8319.
6. Mansour, S. L., Thomas, K. R. & Capecchi, M. R. (1988) *Nature (London)* **336**, 348–352.
7. Doetschman, T. C., Eistetter, H., Katz, M., Schmidt, W. & Kemler, R. (1985) *J. Embryol. Exp. Morphol.* **87**, 27–45.
8. Nagy, A., Rossant, J., Nagy, R., Abramow-Newerly, W. & Roder, J. C. (1993) *Proc. Natl. Acad. Sci. USA* **90**, 8424–8428.
9. McBurney, M. W., Sutherland, L. C., Adra, C. N., Leclair, B., Rudnicki, M. A. & Jardine, K. (1991) *Nucleic Acids Res.* **19**, 5755–5761.
10. Yagi, T., Ikawa, Y., Yoshida, K., Shigetani, Y., Takeda, N., Mabuchi, I., Yamamoto, T. & Aizawa, S. (1990) *Proc. Natl. Acad. Sci. USA* **87**, 9918–9922.
11. Walsh, F. S. & Dickson, G. (1989) *BioEssays* **11**, 83–88.
12. Probstmeier, R., Bilz, A. & Schneider-Schaulies, J. (1994) *J. Neurosci. Res.* **37**, 324–335.
13. Duband, J.-L., Dufour, S., Hatta, K., Takeichi, M., Edelman, G. & Thiery, J. P. (1987) *J. Cell Biol.* **104**, 1361–1374.
14. Kintner, C. (1988) *Neuron* **1**, 545–555.
15. Probstmeier, R., Kuhn, K. & Schachner, M. (1989) *J. Neurochem.* **53**, 1794–1801.
16. Cole, G. J., Loewy, A. & Glaser, L. (1986) *Nature (London)* **320**, 445–447.
17. Cole, G. J. & Akeson, R. (1989) *Neuron* **2**, 1157–1165.
18. Friedlander, D. R., Milev, P., Karthikeyan, L., Margolis, R. K., Margolis, R. U. & Grumet, M. (1994) *J. Cell Biol.* **125**, 669–680.
19. Kadmon, G., Kowitz, A., Altevogt, P. & Schachner, M. (1989) *J. Cell Biol.* **110**, 193–208.
20. Williams, E. J., Furness, J., Walsh, F. S. & Doherty, P. (1994) *Neuron* **13**, 583–594.